

The V_{15} Molecule, a Multi-Spin Two-Level System: Adiabatic LZS Transition with or without Dissipation and Kramers Theorem

Bernard BARBARA,¹ Irinel CHIORESCU^{1,*}
Wolfgang WERNSDORFER,¹ Hartmut BOGGE² and Achim MULLER²

¹*Laboratoire de Magnetisme Louis Néel, CNRS, BP 166, 38042-Grenoble, France*

²*Fakultat fur Chemie, Universitat Bielefeld, D-33501 Bielefeld, Germany*

(Received April 1, 2002)

The so-called V_{15} compound, of formula $K_6[V_{15}^{IV}As_6O_{42}(H_2O)]8H_2O$, is formed of 15 spins $\frac{1}{2}$ antiferromagnetically coupled. The resultant spin is equal to $\frac{1}{2}$. Contrary to what is expected at first sight, this half-integer spin is gapped. We show that this is a consequence of the multi-spin character of the molecule. Time reversal symmetry (Kramers theorem) is preserved due to the existence of a groundstate degeneracy larger than 2. Magnetization experiments have been performed at different temperatures, sweeping-field rates and couplings with the cryostat. Their interpretation in terms of the Landau-Zener-Stückelberg model gives evidence for adiabatic LZS spin reversal with and without dissipation.

§1. Introduction

Contrary to high spin molecules such as Mn_{12} or Fe_8 ($S = 10$),¹ the V_{15} molecule has a low resultant spin ($S = \frac{1}{2}$). This leads to important differences with respect to high spin molecules. In particular, energy barrier between spin-up and spin-down directions, as well as dipolar couplings between molecules, become negligibly small. Nevertheless, in low spin molecules such as V_{15} , the Hilbert space is as huge as in large spin molecules. This is simply because they are both multi-spins. In V_{15} the Hilbert space dimension is equal to 2^{15} ; in Mn_{12} and Fe_8 it is 10^8 and 6^8 respectively. In principle, this molecule should be discussed in terms of the entanglement of the 15 spins $\frac{1}{2}$. However, considerable simplifications occur at low temperature. The groundstate spin is equal to $\frac{1}{2}$ and the first excited one is equal to $\frac{3}{2}$. These levels being reasonably well separated in energy, low temperature experiments deal with the groundstate only. We showed experimentally that in zero field, the symmetric and antisymmetric superposition of the groundstates $|\frac{1}{2}, S_z = \frac{1}{2}\rangle$ and $|\frac{1}{2}, S_z = -\frac{1}{2}\rangle$ are split by an energy Δ . The origin of this splitting with a half-integer spin is attributed to its multi-spin origin. In the absence of decoherence, and in zero field, the ensemble of molecules should coherently oscillate between the symmetric and antisymmetric states $|\frac{1}{2}, S_z = \frac{1}{2}\rangle \pm |\frac{1}{2}, S_z = -\frac{1}{2}\rangle$ with the frequency Δ/h . In the presence of a sweeping field $v_H = dH/dt$, the initial state $|\frac{1}{2}, S_z = \frac{1}{2}\rangle$ either rotates to the state $|\frac{1}{2}, S_z = -\frac{1}{2}\rangle$ or is not modified, depending on the sweeping field rate. The switching probability depends on the comparison of the time $\tau_{sw} = \Delta/v_H g \mu_B$ during which the field sweeps the mixing region ($\sim \Delta/g \mu_B$), with the oscillation

^{*}) Present address: Delft University of Technology, Dept. of Applied Physics, 2628 CJ Delft, The Netherlands.

time $\tau_{os} = \hbar/\Delta$. When the field changes slowly ($v_H \ll \Delta^2/\hbar g\mu_B$) the system stays in the same state (groundstate) and the spin rotates on an adiabatic way from $|\frac{1}{2}, \frac{1}{2}\rangle$ to $|\frac{1}{2}, -\frac{1}{2}\rangle$. When the field changes rapidly ($v_H \gg \Delta^2/\hbar g\mu_B$) the system has not the time to experience quantum mixing and the spin does not rotate. The switching field probability is given by $P = 1 - \exp(-\Gamma)$ with $\Gamma = \pi\Delta^2/2\hbar v_H g\mu_B$. This is the main result of the Landau-Zener-Stückelberg (LZS) without dissipation. This model was introduced for inter-band tunneling in semiconductors.²⁾ It has been recently applied to the specific case of mesoscopic magnetism by Miyashita.³⁾ The effects of dissipation have been considered by several authors.⁴⁾

Our time resolved magnetization measurements performed at different conditions of field, temperature and coupling with the cryostat, are interpreted on the basis of a LZS model. Following Abragam and Bleaney, we introduced the role of phonons and spins through simple spin-phonon and spin-spin transitions.⁵⁾

After this introduction, the paper is ordered as follows: §2 Structural and thermodynamic magnetic properties, §3 Time resolved magnetization measurements, §4 Quantitative approach and evidence for gapped of half-integer spin, §5 Origin of the gap in the V₁₅ molecule, §6 Conclusion.

§2. Structural and thermodynamic magnetic properties

The so-called V₁₅ molecule is a complex of formula $K_6[V_{15}^{IV}As_6O_{42}(H_2O)]8H_2O$. This complex forms a lattice with trigonal symmetry ($a = 14.029\text{\AA}$, $\alpha = 79.26^\circ$, $V = 2632\text{\AA}^3$), containing two V₁₅ complexes per cell. The third order symmetry axis of the unit-cell is also the symmetry axis of the V₁₅ clusters (space group R3-c). All the fifteen V^{IV} ions of spin $S = \frac{1}{2}$ are placed in a quasi-spherical layered structure formed of a triangle sandwiched between two non-planar hexagons (Fig. 1).

There are five antiferromagnetic exchange constants. Each hexagon contains three pairs of strongly coupled spins ($J = 800$ K) and each spin at a corner of the inner triangle is coupled to two of those pairs (one belonging to the upper hexagon and one belonging to the lower hexagon). We have two different determinations of the exchange couplings shown in Fig. 1: $J_1 = J' = -30$ K, $J_2 = J'' = -180$ K, $J = -800$ K⁶⁾ or $J_1 = J' = -150$ K, $J_2 = J'' = -300$ K, $J = -800$ K.⁷⁾ These values should not be taken as definitive. There are too many free parameters in these evaluations. However, the orders of magnitude are correct. The V₁₅ molecule can be seen as formed by three groups of five V^{IV} ions. Each group with a resultant spin $\frac{1}{2}$ is located on a corner of the inner triangle. These three spins $\frac{1}{2}$ interact with each other through two main paths, one passing by the upper hexagon and one passing by the lower one. They are related to each other by the threefold symmetry axis of the molecule. This is a typical example of a frustrated molecule.

The magnetization measurements given below were obtained on single crystals of the V₁₅ complex. A small dilution refrigerator allowing measurements above 0.1 K was inserted in an extraction magnetometer providing fields up to 16 T, with low sweeping rates of about 1 minute/point. Below 0.9 K we clearly observed three jumps, one in zero field, and two at $H_1 = \pm 2.8$ T (Fig. 2). They correspond to the

$-\frac{1}{2} \Leftrightarrow \frac{1}{2}$ and $\pm\frac{1}{2}$ to $\pm\frac{3}{2}$ spin transitions, with respective saturation at $0.50 \pm 0.02\mu_B$ and $2.95 \pm 0.02\mu_B$ per V_{15} molecule. Above 1 K, the observed jumps vanish because the $S = \frac{3}{2}$ level becomes thermally occupied. The magnetization curves are reversible and do not show anisotropy when the field is applied along different directions, within the accuracy of the experiments. Furthermore, experiments made on a single crystal or on several non-oriented single crystals were the same. So, any energy barrier preventing spin reversals must be quite small (less than 50 mK). The magnetization curves measured at equilibrium (Fig. 2) are fitted using the Heisenberg Hamiltonian for three frustrated spins $S = \frac{1}{2}$:

$$H = - \sum_{\alpha=x,y,z} J_{\alpha}(S_{\alpha 1}S_{\alpha 2} + S_{\alpha 2}S_{\alpha 3} + S_{\alpha 3}S_{\alpha 1}) - g\mu_B \mathbf{H}(\mathbf{S}_1 + \mathbf{S}_2 + \mathbf{S}_3), \quad (1)$$

where $S_1 = S_2 = S_3 = \frac{1}{2}$, $J_{\alpha} < 0$ and $g = 2$. The three spins $\frac{1}{2}$ represent the resultant spin of the three groups of five spins (Fig. 1).

The energy scheme for the lowest levels is obtained by diagonalization of the 3-spins matrix of the Hamiltonian (1). This matrix contains 64 terms, and the chosen basis is: $\{|+++\rangle, |++-\rangle, |+-+\rangle, | -++\rangle, |+--\rangle, |+- -\rangle, | -+-\rangle, | - - -\rangle\}$. In the isotropic case and in zero field, the first excited level with spin $\frac{3}{2}$ has, as expected,

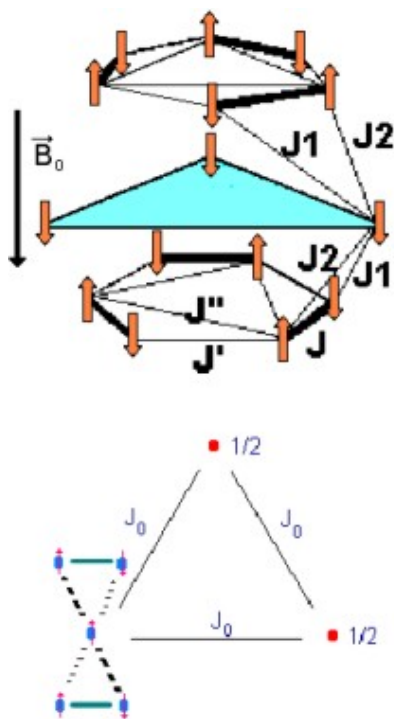


Fig. 1. Quasi-spherical layered structure formed of a triangle of V^{IV} sandwiched between two non-planar hexagons. Main exchange paths have been indicated. Scheme of the 5 spins model used for our calculations.

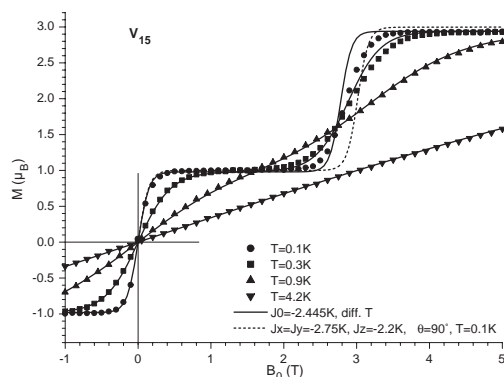


Fig. 2. Magnetization curves measured on a single crystal of V_{15} . The agreement with the calculated curves obtained with our 5-spins model is excellent for $J_0 = -2.445$ K (continuous curves). However, the spin transition measured at 2.8 T and at low temperature is broader than the calculated one. Anisotropic exchange interactions do not influence the shape of the transition (dashed curve for $J_x = J_y = -2.75$ K, $J_z = -2.2$ K). This could be done by antisymmetric D-M interactions.

a fourfold degeneracy. However, it turns out that the ground state, with spin $\frac{1}{2}$, has also a fourfold degeneracy. This is a consequence of its multi-spin character: the groundstate of V_{15} is made of the juxtaposition of two independent spins $\frac{1}{2}$, each with a degeneracy of 2. We will see below that this “degeneracy doubling” effect has a general consequence on the quantum reversal of a spin $\frac{1}{2}$ and more generally of a half-integer spin, if interactions are antisymmetric. It is easy to see analytically that the separation between the ground state and the first excited state is $-3J_0/2$, and that the value of the field at which the configuration $S = S_Z = \frac{3}{2}$ becomes favorable against the $S = S_Z = \frac{1}{2}$ is $H_1 = -3J_0/(2g\mu_B)$. The measured field $H_1 = 2.8$ T gives $J_0 \approx -2.51$ K and then a separation of ≈ 3.76 K. These results are confirmed by high temperature susceptibility experiments (see below). The value of ≈ 3.76 K is extremely small, compared to the exchange interactions J_1, J_2, J . This is a consequence of the spin frustration of the molecule. The three spins $\frac{1}{2}$ of the sandwiched triangle are coupled via the two hexagons, as indicated in Fig. 1. According to this scheme, the exchange fields at the site of each triangle spin should cancel each other. The observed small value of J_0 results from the exchange couplings J_1 and J_2 not cancelling each other exactly. This is why the separation between the lowest levels $S = \frac{1}{2}$ and $S = \frac{3}{2}$ is almost two orders of magnitude smaller than these interactions. The magnetization is calculated from the projection of the magnetic moments upon the applied field $S_{Zi} = \langle i | S_{Z1} + S_{Z2} + S_{Z3} | i \rangle$, averaged over the different eigenvectors $|i\rangle$ of energies E_i . The population of different energy levels is taken at equilibrium (Boltzmann distribution). In the isotropic case, an analytical form of the magnetization is obtained.⁸⁾

The fit of the magnetization curves measured at different temperatures gives $J_0 \approx -2.445$ K, which is very close to the value of 2.51 K independently obtained above. The agreement between calculated and measured curves is excellent at each temperature, except for the slope of the transition at 2.8 T which is broader in experiments. This broadening of about 0.7 T, does not depend on samples and cannot be ascribed to dipolar or hyperfine field distributions (about 1 mT and 40 mT respectively), nor to anisotropy exchange effects included in some of our calculations. However, we found that antisymmetric Dzyaloshinsky-Moriya interactions $\mathbf{D}_{DM} (\mathbf{S}_i \times \mathbf{S}_j)$ (Ref. 9) and references therein), which are allowed by symmetry and couple the states $S = \frac{1}{2}$ and $S = \frac{3}{2}$, might explain this broadening (see §5). In fact the important effect of Dzyaloshinsky-Moriya interactions for the induction of tunnel splittings, otherwise forbidden, was pointed out in Ref. 10) for the case of the Mn_{12} molecule. Detailed calculations have been done in Ref. 11).

The susceptibility is calculated by taking the first derivative of the analytical expression of the magnetization.⁸⁾ The zero-field susceptibility χ_i has a very simple expression:

$$\chi_i = (g\mu_B)^2 \frac{(5 + e^{-3J_0/2kT})}{4kT(1 + e^{-3J_0/2kT})}. \quad (2)$$

The limits $T \ll 3J_0/2k$ and $T \gg 3J_0/2k$ correspond respectively to a spin $\frac{1}{2}$ with the effective moment $\sqrt{3}g\mu_B/2$, and 3 spins $\frac{1}{2}$ with the effective moment $3g\mu_B/2$. The fit of the susceptibility curves measured between 0.1 K and 100 K is given Figs. 3

and 4. The measured reciprocal susceptibility vs temperature and its comparison with Eq. (2) for $J_0 \approx -2.445$ K (determined from $M(H)$) is excellent. The straight line represents the Curie-Weiss law with the Curie constant $C = 0.686\mu_B K/T$ and the paramagnetic temperature $\theta = -12$ mK. This Curie constant corresponds to the effective paramagnetic moment $1.75\mu_B$, a value very close to $g\mu_B(S(S+1))^{1/2} = g\mu_B\sqrt{3}/2$ for $S = \frac{1}{2}$. The paramagnetic Curie temperature is of the order of dipolar couplings between $S = \frac{1}{2}$ molecule spins. Above 0.5 K, the susceptibility deviates from the experimental data and from the calculation from Eq. (2). This is because the spin $\frac{1}{2}$ ground-state starts to be deteriorated. Figure 4 shows the measured effective moment $\mu_{\text{eff}} = \sqrt{3kT\chi_i}$ as a function of temperature. It increases from the value of $1.75\mu_B$ corresponding to the spin $\frac{1}{2}$ ground state, and tends asymptotically to the value of $3\mu_B$ which is preserved up to 100 K (three independent spins $\frac{1}{2}$). The fit of these susceptibility measured between 0.1 and 125 K to Eq. (2) is excellent with $J_0 = -2.445$ K.

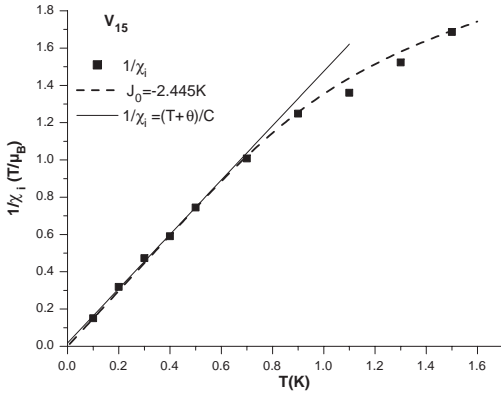


Fig. 3. Measured and calculated reciprocal susceptibility vs temperature. The dashed curve comes from the model with $J_0 = -2.445$ K and the continuous line is a Curie-Weiss fit with a paramagnetic Curie temperature $q = 12$ mK and a Curie constant corresponding to an effective moment of 1.75 mB ($S = \frac{1}{2}$).

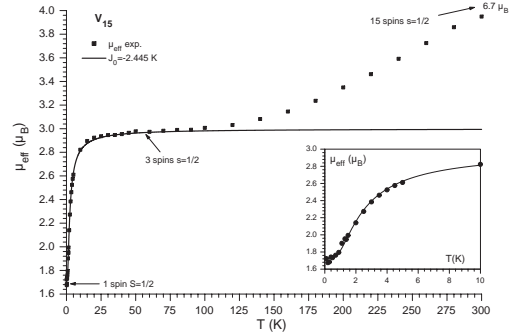


Fig. 4. Curve calculated in the 5-spins model is valid up to 125 K, showing that excited levels corresponding to triangle-hexagons couplings are well separated from the triangle levels. Two plateaus can be seen: one at 1.75 mB corresponding to one spin $\frac{1}{2}$ (below 0.5 K) and one at 3 mB corresponding to three spins $\frac{1}{2}$ (above 25 K).

§3. Study of the two-level system realized in the V_{15} molecule

In this section we concentrate on the zero-field $|\frac{1}{2}, S_z = \frac{1}{2}\rangle \Leftrightarrow |\frac{1}{2}, S_z = -\frac{1}{2}\rangle$ transition. We studied the temperature and time dependence of a small single-crystalline grains of V_{15} ($L \approx 30 - 40 \mu\text{m}$), with different couplings to the cryostat. A first comparison with the LZS model shows that with zero-field splitting of the order of $50 - 200$ mK (see §4) the transition is purely adiabatic if $v_H \ll 10^{10}$ T/s. In our experiments where $v_H \leq 0.14$ T/s (see below) it is a fortiori the case. Our experiments being done at finite temperatures, we found a much richer behavior than

simple adiabatic LZS, with two limiting cases in which the magnetization curves $M(H)$ are reversible, and an intermediate one where it is irreversible. This behavior results from effects of the environment on the adiabatic LZS model.

3.1. *Fast sweeping rate / weak coupling to the cryostat, and adiabatic LZS*

The first limit of fast field variations and weak coupling to the cryostat, was reached by inserting a plastic sheet, much thicker than the sample, between the sample and the sample-holder and restricting the temperature to lowest values. The four $M(H)$ curves of Fig. 5 show either a weak hysteresis or no hysteresis at all, depending on the competition of temperature (giving hysteresis through spin-phonons transitions) and sweeping field rate $v_H = dH/dt$ (preventing these transitions). This effect can be accounted for by the ratio $\alpha v_H/T^2$ (see the model below). For $\alpha v_H/T^2 < 14 \text{ T/sK}^2$ weak hysteresis is observed on the $M(H)$ curve. It is attributed to finite but small probability for spin-phonon transitions. For $\alpha v_H/T^2 > 14$ to 40 T/sK^2 the $M(H)$ curve becomes reversible. Spin-phonons transitions have not the time to take place and the probability for their occurrence is negligibly small; only the groundstate is occupied. The $|\frac{1}{2}, S_z = \frac{1}{2}\rangle$ to $|\frac{1}{2}, S_z = -\frac{1}{2}\rangle$ LZS transition is adiabatic. The adiabatic $M(H)$ curve is nicely fitted with the expression $M = (\frac{1}{2})(g\mu_B)^2 H / [(\Delta_0)^2 + (g\mu_B H)^2]^{\frac{1}{2}}$ obtained from $E = \frac{1}{2} d\Delta_H/dH$ where $\Delta_H = [(g\mu_B H)^2 + (\Delta_0^2)]^{\frac{1}{2}}$ is the two-level field-dependent splitting energy. The saturation $(\frac{1}{2})g\mu_B$ is very close to $1\mu_B$ as expected, and the initial slope $M/H = (g\mu_B)^2/2\Delta_0$ is proportional to $1/\Delta_0$, giving immediately an order of magnitude for the zero-field splitting $\Delta_0 \approx 0.1 \text{ K}$. The fit of the whole $M(H)$ curve, as well as the $1/H^2$ approach to saturation gives $\Delta_0 \approx 80 \text{ mK}$.

In short, a single crystal of V_{15} molecules with reduced couplings to the cryostat, is a realization of the adiabatic LZS model applied to magnetism.³⁾ The spin temperature can then reach very low values $T_s = T_i/(1 + (g\mu_B H/\Delta_0)^2) \approx T_i/50$, where T_i is the initial temperature. The same procedure applied to the $\frac{1}{2}$ to $\frac{3}{2}$ spin transition which occurs in a rather high field (2.8 T) should allow to obtain high nuclear spins polarization.

3.2. *Low sweeping rate / strong coupling to the cryostat, and dissipative LZS*

Here the coupling between the sample and the cryostat is made better in order to favor spin-phonons transitions. We considered two cases. In the first one, the coupling was obtained by simple contact using some grease between sample and sample holder. In the second case the coupling was better, the contact being made of a mixture of silver powder with grease. In both cases non-equilibrium hysteresis loops are observed at fast-sweeping rate, down to the lowest measured temperature of 50 mK.

The $M(H)$ curves obtained with the first type of coupling (grease contact), can be found in Refs. 8), 9) and 13). Those obtained with the best coupling with the cryostat (Ag+grease) are similar. They are shown Fig. 6. When the field increases, coming from negative values, the magnetization passes through the origin of the coordinates, reaches a plateau and then approaches saturation. This leads to

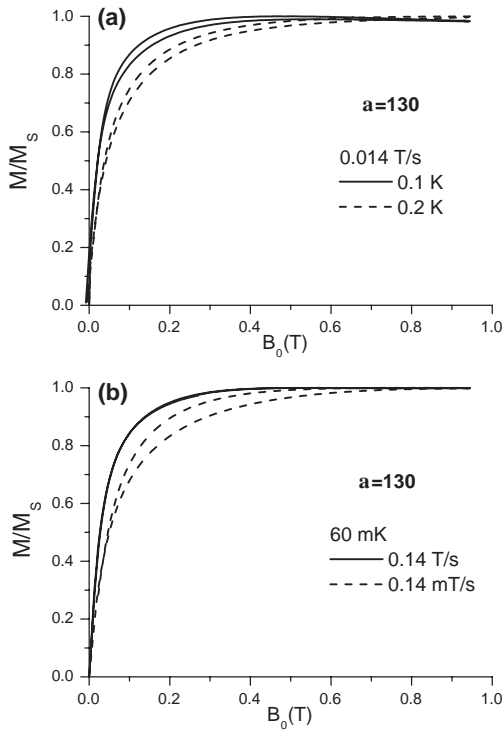


Fig. 5. Hysteresis loops measured in the case of a sample rather well isolated from the cryostat ($\alpha = 130 \text{ sK}^2$). The curve at 60 mK and 0.14 T/s shows an adiabatic LZS spin transition. It is very well fitted with the expression $\frac{M}{M_s} = \frac{d\Delta_H}{dH}$.

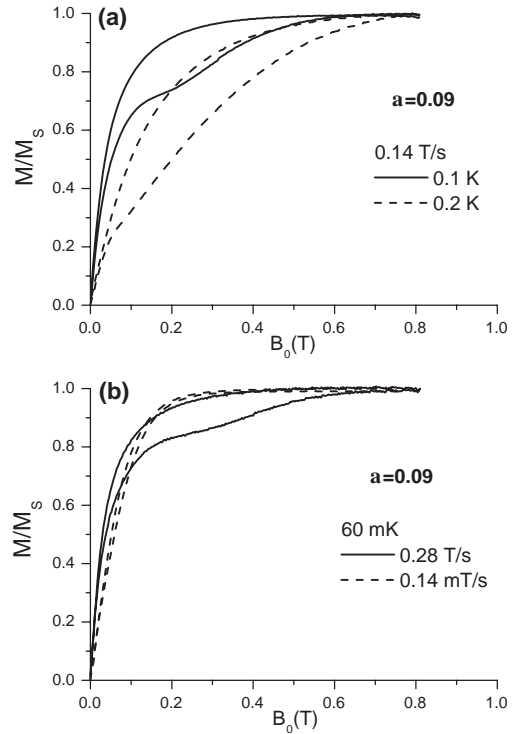


Fig. 6. Hysteresis loops measured in the case of a sample rather well coupled to the cryostat ($\alpha = 0.09 \text{ sK}^2$).

a winged hysteresis loop characterized by a reversible but temperature and sweeping field-dependent zero-field susceptibility. The irreversible wings depend also on temperature and sweeping field. The sweeping field dependence of the zero-field susceptibility is typical of the phenomenon studied here.

In Fig. 6 the hysteresis of the $M(H)$ curves disappears when the field is slow enough. This is a natural consequence of thermal equilibrium. Spin-phonons transitions are sufficiently probable so that the two-level populations equilibrate with the Boltzmann distribution. As an example, equilibrium is almost reached at 60 mK and $v_H < 0.14 \text{ mT/s}$ (approximated by the median of the two branches of the $M(H)$ hysteresis loop, Fig. 6). This reversibility is very different from the one discussed in §3.1. where field variations were fast enough to suppress spin-phonons transitions completely, giving a highly non-equilibrium groundstate at finite temperature (adiabatic LZS).

In order to give a first qualitative analysis of these “butterfly hysteresis loops”⁹⁾ we will see how the level occupation numbers vary when sweeping the external field (Fig. 7). The spin temperature T_S is such that $n_1/n_2 = \exp(\Delta_H/k_B T_S)$ where

$n_{1,2}$ ($n_{1,2\text{equ}}$) is the out of equilibrium (equilibrium) level occupation numbers. The magnetization curves at 60 mK (Fig. 6, Refs. 8), 9) and 13)), show a spin temperature significantly lower than the bath temperature ($n_1 > n_{1\text{equ}}$, $T_S < T$) between 0.3 T and 0.15 T (the field at which the magnetization curve intersects the equilibrium one). After this intercept, T_S is larger than the bath temperature ($n_1 < n_{1\text{equ}}$, $T_S > T$) and at sufficiently high fields (about 0.5 T) it reaches its equilibrium value ($n_1 = n_{1\text{equ}}$, $T_S = T$). Note that the magnetization curves measured between 0.7 and 0.02 T at fast sweeping rates are nearly the same, suggesting weak exchange with the bath, i.e. nearly adiabatic demagnetization. This is because below 0.5 K, the heat capacity of phonons C_{ph} is very much smaller than that of the spins C_S , so that the phonons temperature T_{ph} very rapidly adjusts to that of the spins T_S . The spins and the phonons can be seen as a single system. The coupling of this system with the cryostat is weak because energy transfers through phonons must obey the drastic condition $\hbar\omega = \Delta_H$ and the number of phonons available at this energy $\hbar\omega$ is extremely small: $n_T = \int \sigma(\omega)d\omega / \exp(\hbar\omega/kT)$. The integral is taken over the level linewidth $\Delta\omega$ (due to fast hyperfine fluctuations), $\sigma(\omega)d\omega = 3V\omega^2d\omega/2\pi v_{\text{ph}}^3$ is the number of phonon modes between ω and $d\omega$ per molecule of volume V , and v_{ph} is the phonon velocity. Taking the typical values for V_{15} like systems $v = 3000$ m/s, and $\Delta\omega = 10^2$ MHz, we find at $T = 0.1$ K, $n_T \approx 10^{-6} - 10^{-8}$ phonons/molecule. The number of such lattice modes being much smaller than the number of spins, energy transfer between phonons from the cryostat and spins must be very difficult, a phenomenon known as the phonon bottleneck.^{5), 12)} Despite a good thermal contact between the sample and the cryostat, the energy flow from the latter is not sufficient to compensate the lack of phonons at energies $\hbar(\omega \pm \Delta\omega)$. Most molecules are out of equilibrium, at a temperature T_s different from the cryostat temperature T .

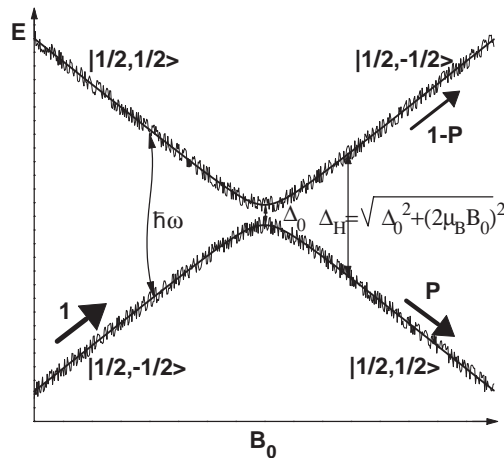


Fig. 7. Schematic representation the V_{15} spin $\frac{1}{2}$ energy scheme in a magnetic field. Probability transitions P in the LZS model and spin-phonons transitions are indicated by different types of arrows. The existence of a zero-field splitting Δ_0 with a spin $\frac{1}{2}$ is related to the fact that in V_{15} , this scheme is doubly degenerated with the superposition of two independent and identical schemes.

§4. Quantitative approach and numerical calculations

In a spin $\frac{1}{2}$ two-level system, the populations of spins and phonons obey a set of two differential equations given by Abragam and Bleaney.⁵⁾ As discussed above, at low enough temperature, the condition $b = C_s/C_{\text{ph}} \gg 1$ implies $T_{\text{ph}} \rightarrow T_s \neq T$. The phonon population is dragged by that of the spins, and the problem reduces to a single equation. Writing $x = (n_1 - n_2)/(n_{1\text{eq}} - n_{2\text{eq}})$, the spin population is given by $\tau_H dx/dt = 1/x - 1$. The solution of this simple equation is $-t/\tau_H = x - x_0 + \ln[(x - 1)/(x_0 - 1)]$ where $\tau_H = b\tau_{\text{ph}} = (\alpha/\Delta_H^2) \tanh^2(\Delta_H/2k_B T)$ is the relaxation time of the spin-phonon system to the cryostat temperature and x_0 the initial spin population. The constant α is formally proportional to the size L of the sample, i.e. to the distance the phonons have to travel to reach the cryostat temperature.⁹⁾ In experiments, it is common to change L artificially by modifying the thermal coupling at the sample/sample-holder interface (see above). The above expressions of x and τ_H allow to calculate the magnetic relaxation and the magnetization curves $M(H, T, t)$ with the use of only two parameters Δ_0 and α . Note that $\tau_H dx/dt$ could be written $\tau_H v_H (dx/dH)$, suggesting that the parameter $\tau_H v_H \propto \alpha v_H/T^2$ is relevant for $M(H)$ curves.

The $M(H)$ curves have been calculated to give the best agreement with the measured ones. The obtained parameters are $\Delta_0 \approx 50$ mK and $\alpha \approx 0.15$ sK² (grease contact). The comparison between the magnetic relaxation curves measured in the same conditions and calculated (not shown) gives $\Delta_0 \approx 150$ mK. In the case of the best coupling between sample and cryostat, the agreement between measured and calculated $M(H)$ curves gives $\Delta_0 \approx 80$ mK and $\alpha \approx 0.09$ sK². This smaller value of α is consistent with a better contact to the cryostat. These determinations of Δ_0 must be compared to the value $\Delta_0 \approx 80$ mK obtained from the fit of $M(H)$ without dissipation (§3.1). Relaxation time measurements being less accurate than $M(H)$ fits, we can consider that the zero-field splitting of V_{15} is $\Delta_0 \approx 80 \pm 20$ mK.

Although these quantitative determinations of Δ_0 are not direct (neutron scattering experiments are in progress), the obtained finite value is qualitatively proved by the sweeping field dependence of the initial susceptibility and in particular by the clear observation of an adiabatic LZS regime, in fast fields. Quantitatively, the value of about 80 mK seems rather safe for the following reasons. We obtained three couples (Δ_0, α) independently from the comparison of measured and calculated $M(H)$ curves in the adiabatic LZS regime without dissipation (bad coupling with the cryostat, $\alpha \approx 130$ sK²) and with dissipation (good and very good couplings, $\alpha \approx 0.15$ and 0.09 sK²). The Δ_0 values obtained are close to each other and the values are consistent with the whole physical picture, giving credit to our

Table I. Relaxation times at different fields and temperatures, obtained from the fit of the curves shown Fig. 8 ($\tau_{H\text{exp}}(\text{s})$) and calculated from the time dependent equation given in the text with $\alpha = 130$ sK² and $\Delta_0 = 80$ mK.

$T(\text{K})$	$H(\text{mT})$	$\tau_{H\text{exp}}(\text{s})$	$\tau_{H\text{calc}}(\text{s})$
0.05	14	1507	8716
0.15	14	551	1323
0.05	70	3883	3675
0.15	70	970	997

approach. Furthermore, our model is self-consistent. In the case of $\alpha \approx 0.15 \text{ sK}^2$ we have found a relaxation time of about 1s, from the above expression of τ_H , which is close to the measured one.¹³⁾ Moreover, we obtained (i) a sound velocity $v_{\text{ph}} \approx 3000 \text{ m/s}$, which corresponds to the values given for insulating systems,⁵⁾ and (ii) the calculated specific heat ratio $b = \tau_H v_{\text{ph}} / L \approx 10^8$ is comparable to the expected value for an ensemble of spins $\frac{1}{2}$ in a low temperature bottleneck regime.^{5), 12)} Finally, in the other limit where $\alpha \approx 130 \text{ sK}^2$ and $\Delta_0 \approx 80 \text{ mK}$, our magnetic relaxation measurements are well fitted to the model given above and the obtained relaxation times are very close to the calculated ones for the whole range of fields, excepted near zero field where the measured relaxation (Fig. 8) is about six times faster (Table I). This shows that when the relaxation takes place within the zero-field splitting Δ_0 , the phonons bath is no longer sufficient to explain the dissipation. An excess relaxation probably comes from the Dzyaloshinsky-Moriya interactions and the spin-bath and in particular from the fast fluctuations of the ^{51}V nuclear spins. A more detailed study of the interplay between nuclear and electronic spins, in the presence of the spin mixing of the Dzyaloshinsky-Moriya interactions should be done in the case of this molecule, in the light of our recent works on H_0^{3+} ions.¹⁴⁾ For a discussion see the next section.

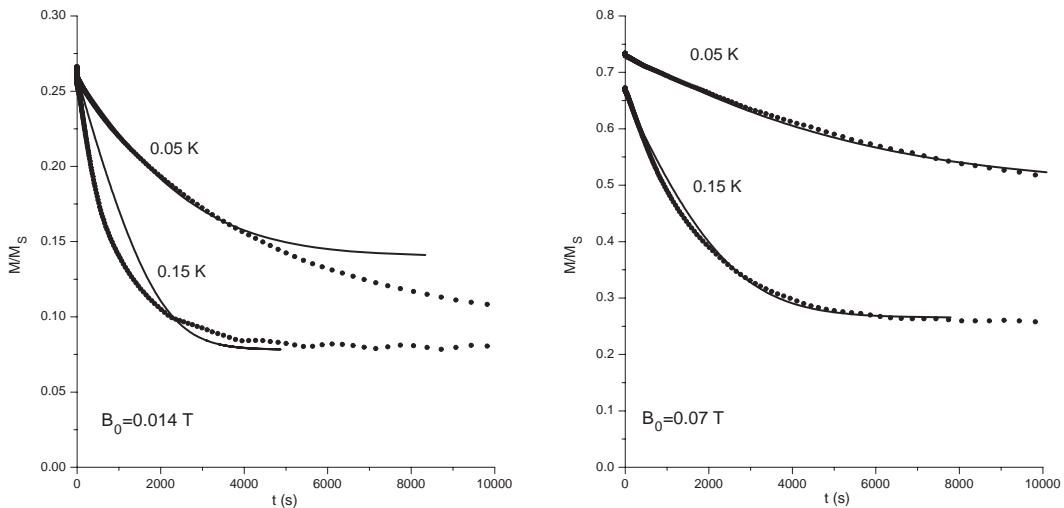


Fig. 8. Relaxation of an isolated sample, in a field $H \ll \Delta_0$ for which spin up and spin down states are mixed (left), and in a field $H \gg \Delta_0$ where the level structure is dominated by the Zeeman effect. The fits (continuous curves) of data (dots) are good except when the field and the temperature are small (0.15 K, 0.014 T).

§5. Origin of the gap in the half-integer $\frac{1}{2}$ spin of the V_{15} molecule

It is well known that time reversal symmetry prevents half-integer spins to be gapped in zero field (Kramers theorem¹⁵⁾). This is also the reason for the absence of Haldane gap in magnetic chains with half-integer spins.¹⁶⁾ Our first evidence for a gap in spins $\frac{1}{2}$ V_{15} molecules is at first sight in contradiction with this first principle. The

difference between the spin $\frac{1}{2}$ of V_{15} and an atomic spin $\frac{1}{2}$ is obviously the multi-spin character of V_{15} . The groundstate spin $\frac{1}{2}$ is the resultant of exchange interactions as shown §2. As we suggested in Ref. 9) and references therein, antisymmetric Dzyaloshinsky-Moriya (D-M) interactions can provide a finite gap in a multi-spin system with resultant half-integer spin. On the point view of symmetry, the molecule V_{15} is a good candidate to show this effect, due to the lack of inversion center. This is particularly true for spin pairs situated near the borders of the molecules. The Hamiltonian (1) should therefore contain the additional term:

$$H = - \sum_{ij} \mathbf{D}_{ij} \mathbf{S}_i \times \mathbf{S}_j, \quad (3)$$

the summation being done over all spin pairs. The norm of the vector \mathbf{D} can be evaluated from the measured anisotropy of the g -factor. Very recent EPR experiments by Ajiro et al.¹⁷⁾ made accurate measurements of the angular variations of this factor, in a plane containing the c -axis. The results, much more complete than the previous ones,^{6),7)} give at 2.4 K, $g_{\parallel c} = 1.98$ and $g_{\perp c} = 1.968$. Then using $D \approx J\Delta g/g$, with $\Delta g/g = (g_{\parallel c} - g_{\perp c})/g = 0.6\%$, we can see that the value $DS^2 \approx D/4 \approx 80$ mK derived from measured Δ_0 , gives $J \approx 60$ K, which is of the right order of magnitude for average exchange interactions. Therefore D-M interactions could really be at the origin of the observed zero-field splitting. We do not see what else could give this effect.

The best theoretical proof for that was given recently by Miyashita and Nagaosa¹⁸⁾ who calculated the magnetization curves and splittings resulting from level mixings in the 3-spins Heisenberg model (Hamiltonian (1) in §2) with various types of perturbations of the form

$$H_1 = - \sum_{i,j} \alpha_{ij} S_{iz} S_{jx}. \quad (4)$$

They showed that the groundstate is not gapped, as expected from the Kramers theorem,¹⁵⁾ only if the α_{ij} show the reflection symmetry, i.e. $\alpha_{ij} = \alpha_{ji}$. In other cases, when $\alpha_{ij} \neq \alpha_{ji}$ the perturbation (4) removes the spins $\frac{1}{2}$ degeneracy. However, as discussed above, the spin $\frac{1}{2}$ being a multi-spin system, its groundstate degeneracy is larger than 2. In the present case of 3 spins $\frac{1}{2}$ it is equal to 4. The four states with $S = \frac{1}{2}$ form two sets of avoided level crossing at zero field, each with two-fold degeneracy. This allows Kramers time reversal symmetry to be preserved even in the presence of a zero-field splitting. Coming back to (3), one can write $H_y = -D_{ijy}(S_{ix}S_{jz} - S_{iz}S_{jx})$, which identifies to (4) if $\alpha_{ij} = -\alpha_{ji} = D_{ijy}$, which is not surprising as D-M interactions are antisymmetric.

Beyond the case of the V_{15} molecule, D-M interactions, which are very general with molecules (and in particular if they are of finite size), should lead to gapped groundstates, even if the multi-spin groundstate is non-integer. It is possible that other mechanisms, such as the multi-exchange couplings in spin liquids, could lead to similar effects. The molecule V_{15} can be considered as an example of nanometer scale spin-liquid.

Before ending this section, let us consider some characteristics¹⁹⁾ of the nuclear spins of ^{51}V . The natural abundance of this element with nuclear spin $\frac{7}{2}$, is 99.76 %. The resonance frequency and magnetogyric ratio of 2.63 GHz and 7.045 rad/ 10^7 T give a hyperfine field of about 40 T. The inverse hyperfine field acting on electronic spins, roughly 2000 times smaller, is in the 20 mK scale, i.e. of the order of $\Delta_0 \approx 80$ mK (if one takes into account the coefficient of $\sqrt{15}$ resulting from random orientations of the 15 nuclear spins of a molecule). As indicated before, this field will give a broadening of electronic levels. This broadening corresponds to the incoherent bunching of 16 electro-nuclear levels. It is important to note that these levels are with integer spins and if their lifetime is larger enough, the change of spin parity due to the hyperfine coupling, should allow the observed zero-field splitting. Another origin for level broadening comes from the spin mixing by Dzyaloshinsky-Moriya interactions between the different pairs of spins in the molecule. The observation of faster relaxation near zero field, suggests that fluctuations on the two levels intercept each other near zero field (at the energy scale of Δ_0). This is the case for nuclear spin fluctuations, the broadening of which is of the order $\Delta_0/2$. These fluctuations should therefore be relevant to explain the excess of relaxation in zero field.^{8), 9), 14)} Level broadening, resulting from incoherent nuclear spins or Dzyaloshinsky-Moriya fluctuations, can be considered as a magnetic external noise on the LZS model.²⁰⁾ Such a noise cannot explain the origin of Δ_0 , in particular because it cannot, by itself, simulate the LZS model, nor the associated dynamics in the presence of spin-phonons transitions. As shown above the origin of Δ_0 is clearly associated with the static antisymmetric effect of Dzyaloshinsky-Moriya interactions.

§6. Conclusion

The V_{15} molecule, a multi-spin system with spin $\frac{1}{2}$, shows clearly adiabatic LZS transitions with or without dissipation, depending on the sweeping field rate and on the coupling with the cryostat. This allows to study environmental effects on quantum spin reversal in a two level system. In particular it is shown that the observed magnetic relaxation is associated with spin-phonons transitions in the Zeeman regime (phonon bath). Near zero field, level broadening due to spin fluctuations (essentially nuclear spin fluctuations) seem to overlap, giving an excess of relaxation, associated with the spin bath. An important consequence of this study is that, contrary to what is expected at first sight, this half-integer spin is gapped in zero-field. This is a consequence of the multi-spin character of the molecule plus Dzyaloshinsky-Moriya interactions. Time reversal symmetry is preserved due to a fourfold degeneracy of the groundstate (larger than 2). This mechanism was verified theoretically. Another possible mechanism to be investigated theoretically is spin parity change due to the hyperfine coupling.

Acknowledgements

B. B. would like to thank the organizing committee of the 16th Nishinomiya-Yukawa Memorial Symposium for their kind invitation, and particularly Professors

T. Tonegawa, H. Takayama and S. Miyashita. We would like to thank them and especially Professors Miyashita and Stamp for discussions on our common field of interest. A. M. thanks the Deutsche forschung genienschalt and European union for financial support.

References

- 1) I. Tupitsyn and B. Barbara, *Magneto-Science-From Molecules to Materials*, ed. M. Drillon and J. Miller (Wiley VCH Verlag GmbH, 2001).
- 2) L. Landau, Phys. Z. Sowjetunion **2** (1932), 46.
C. Zener, Proc. R. Soc. London A **137** (1932), 696.
E. C. G. Stueckelberg, Helv. Phys. Acta **5** (1932), 369.
- 3) S. Miyashita, J. Phys. Soc. Jpn. **64** (1995), 3207.
L. Gunther, Euro. Phys. Lett. **39** (1997), 1.
V. V. Dobrovitski and A. K. Zvezdin, Euro. Phys. Lett. **38** (1997), 377.
- 4) A. J. Leggett, S. Chakravarty, A. T. Dorsey, M. P. A. Fisher, A. Garg and W. Zwerger, Rev. Mod. Phys. **59** (1987), 1.
M. Grifoni and P. Hanggi, Phys. Rep. **304** (1998), 56.
Y. Kayanuma and H. Nakayama, Phys. Rev. B **57** (20) (1998), 13099.
E. Shimshoni and A. Stern, Phys. Rev. B **47** (1993), 9523.
- 5) A. Abragam and B. Bleaney, *Electronic Paramagnetic Resonance of Ions* (Clarendon Press, Oxford, 1970), chap. 10.
- 6) A. L. Barra et al., J. Am. Chem. Soc. **114** (1992), 8509.
- 7) D. Gatteschi et al., Molecular Engineering **3** (1993), 157.
- 8) I. Chiorescu, PhD Thesis, University Joseph Fourier, Grenoble 1 (2000).
- 9) I. Chiorescu, W. Wernsdorfer, A. Muller, H. Bogge and B. Barbara, Phys. Rev. Lett. **84** (2000), 3454.
- 10) B. Barbara, L. Thomas, F. Lioni, A. Sulpice and A. Caneschi, J. Magn. Magn. Mater. **177** (1998), 1324.
- 11) M. I. Katsnelson, V. V. Dobrovitski and B. N. Harmon, Phys. Rev. B **159** (1999), 6919.
- 12) J. H. van Vleck, Phys. Rev. **59** (1941), 724.
- 13) I. Chiorescu, W. Wernsdorfer, A. Muller, H. Bogge and B. Barbara, J. Magn. Magn. Mater. **221** (2000), 103.
- 14) R. Giraud, W. Wernsdorfer, A. M. Tkachuk, D. Mailly and B. Barbara, Phys. Rev. Lett. **87** (2001), 057203-1.
- 15) H. A. Kramers, Proc. Amsterdam Acad. **33** (1930), 959.
- 16) F. D. M. Haldane, Phys. Rev. Lett. **93** (1983), 454; *ibid* **50** (1983), 1153.
- 17) Y. Ajiro et al., to be published.
- 18) S. Miyashita and N. Nagaosa, Prog. Theor. Phys. **106** (2001), 533.
- 19) R. Harris, *Magnetic Resonance in Spectroscopy* **6** (J. Wiley and sons, 1986), p.100.
- 20) K. Saito and S. Miyashita, J. Phys. Soc. Jpn. **70** (2001), 3385.